

A Planar Resonator Antenna Based on a Woodpile EBG Material

Andrew R. Weily, *Member, IEEE*, Levente Horvath, Karu P. Esselle, *Senior Member, IEEE*, Barry C. Sanders, and Trevor S. Bird, *Fellow, IEEE*

Abstract—A resonator antenna made from a complex artificial surface and a metallic ground plane is described. The complex surface is realized using a woodpile electromagnetic bandgap (EBG) material, which is shown to have a frequency dependent reflection plane location. A highly directive radiation pattern is created due to the angle-dependent attenuation of the resonator antenna coupling to free space. The antenna has the advantages of low height, low loss, and low sidelobes. It is shown that the directivity can be varied over a fixed range by changing the aperture size of the device, with the maximum directivity determined by both the feed element and EBG material properties. The complete bandgap for the woodpile EBG material is confirmed from a band diagram, and its properties as a complex surface are investigated through transmission calculation and measurement. The design of the antenna is described, and two means of exciting the resonator, a microstrip patch and a double slot, are investigated. Theoretical results for these two antennas are calculated using finite-difference time-domain and are shown to be in good agreement with measured results.

Index Terms—Electromagnetic bandgap (EBG) material, finite-difference time-domain (FDTD), high gain antenna, resonator antenna, three dimensional (3-D) photonic crystal.

I. INTRODUCTION

ELECTROMAGNETIC bandgap (EBG) materials, also known as photonic crystals, are creating new possibilities for controlling and manipulating the flow of electromagnetic waves. They are formed from dielectric structures that are periodic in one or more dimensions [1]. Within the EBG material there is a range of frequencies where propagating modes can be fully suppressed in one or more dimensions. This range of frequencies is known as the EBG. A complete EBG suppresses propagating modes in all three dimensions, and can only be obtained from a three-dimensional (3-D) photonic

Manuscript received December 15, 2003; revised August 23, 2004. This work was supported in part by an Australian Research Council (ARC) Linkage Post-doctoral Fellowship (CSIRO) and in part by an ARC Discovery Grant. The work of B. C. Sanders was supported by the Alberta informatics Circle of Research Excellence (iCORE) fund.

A. R. Weily and K. P. Esselle are with the Department of Electronics, Macquarie University, Sydney, New South Wales 2109, Australia (e-mail: aweily@ics.mq.edu.au).

L. Horvath was with the Department of Physics, Macquarie University, Sydney, New South Wales 2109, Australia. He is now with the Department of Physics, University of Auckland, 92019 Auckland, New Zealand.

B. C. Sanders is with the Australian Centre for Quantum Computer Technology, Macquarie University, Sydney, New South Wales 2109, Australia, and also with the Institute for Quantum Information Science, University of Calgary, Alberta, ON T2N 1N4, Canada.

T. S. Bird is with Macquarie University, Sydney, New South Wales 2109, Australia, and also with CSIRO ICT Centre, Epping, New South Wales 1710, Australia.

Digital Object Identifier 10.1109/TAP.2004.840531

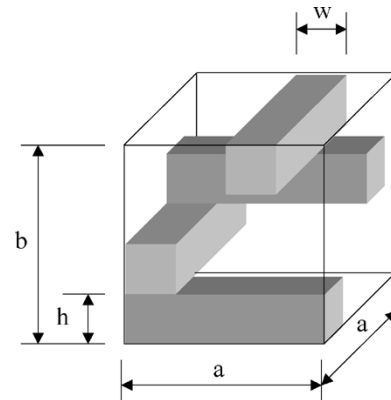


Fig. 1. Unit cell for the woodpile EBG material.

crystal. EBG materials can provide significant advantages for suppressing and directing radiation when used in antennas. Thus far, most research has focused on one-dimensional (1-D) and two-dimensional (2-D) EBG materials because they are easier to construct, but due to their complete bandgap 3-D EBG materials have the potential to give greater control of the radiation properties of antennas.

Many novel antennas based on EBG technology are already finding useful applications [2]. The operating mechanism of these devices can be broadly grouped into the following five classes: 1) EBG substrates and high impedance ground planes that reduce surface waves and increase radiation efficiency [3]–[13], or lower the profile of the design [14], [15]; 2) reflector antennas made from all-dielectric EBG materials or high impedance ground planes [16]–[19]; 3) defect resonator antennas that create high directivity over a narrow bandwidth [20]–[25]; 4) sources embedded in EBG materials that have high directivity due to the limited angular propagation allowed within the material [26]–[28]; and 5) directive EBG horn antennas and arrays that allow efficient coupling from a defect waveguide to free space [29].

In this paper we describe theory and measured results for an antenna made from a woodpile EBG material and a metallic ground plane. The woodpile EBG material is a dielectric structure that is periodic in all three dimensions [30]. This periodicity gives it a wide complete EBG: no propagating modes exist in any direction within the material for frequencies in the bandgap. The woodpile is also referred to as a layer-by-layer photonic crystal in the physics literature. A unit cell of this material is shown in Fig. 1. Through the use of the ground plane with the EBG material the overall height of our prototype is reduced by

more than 70% compared with earlier reported woodpile resonator antennas [24] and this leads to a considerable decrease in the overall volume and weight of the antenna. We provide detailed results on the EBG of the woodpile material and its use as a complex surface for creating a defect resonant cavity.

After discussing the antenna's principle of operation we describe two different configurations of the device: the first uses a microstrip patch feed element to couple energy to and from the resonator, while the second uses a double slot arrangement. Experimental and computed results are presented for the reflection coefficient, radiation patterns, gain and half power beam widths (HPBW) for both structures.

II. WOODPILE EBG MATERIAL

This section provides some background information on the woodpile EBG material, before examining its use in two different planar resonator antenna configurations. The woodpile EBG material (Fig. 1) is defined by the lattice constant or repeat distance in the horizontal plane, a , the rod width w , the rod height h , and the total height of the unit cell b . Notice in Fig. 1 that consecutive layers are orthogonal to each other, and the parallel rods are offset from the rods two layers below by half a lattice constant, to obtain a four layer stacking sequence. The lattice symmetry of this material is face-centered tetragonal (FCT) from solid state physics theory. The cross section of the rods used may be circular or square, and the inverse structure made of air rods in dielectric background also has a complete bandgap.

To implement the woodpile we have used alumina rods ($\epsilon_r = 8.4$, $\tan \delta = 0.002$) that have a rectangular cross section, with lattice parameters of $a = 11.2$ mm, $w = h = 3.2$ mm, and $b = 12.8$ mm. We have calculated the EBG for this woodpile using RSOFT's BandsOLVE commercial software, which implements the plane-wave expansion method [31]. For a numerical grid size of 32 points in each direction, analysis of the unit cell yields a bandgap that extends in normalized frequency from $\omega a/2\pi c = 0.423$ to 0.479 . The gap width to mid-gap ratio is 12.4%. Converting normalized values to real frequency for a lattice constant of 11.2 mm shows that the bandgap of our alumina prototype extends from 11.33 to 12.83 GHz.

The band diagram or dispersion relation computed using BandsOLVE is illustrated in Fig. 2(a), which depicts the first six bands or frequency eigenvalues of the woodpile plotted as a function of the wavevector \vec{k} . The horizontal axis represents 3-D wavevectors, the value of which traces a path around the boundary of the *irreducible Brillouin zone* of the FCT lattice. We show the irreducible Brillouin zone in Fig. 2(b) to clarify this path. The letters that appear on the horizontal axis of Fig. 2(a) correspond to the vertices of the irreducible Brillouin zone shown in Fig. 2(b). The normalized values of the vertices in (k_x, k_y, k_z) format are: X = (0.5, 0, 0.5); U = (0.625, 0.25, 0.375); L = (0.5, 0.5, 0); Γ = (0, 0, 0); W = (0.75, 0, 0.25); and K = (0.75, 0, 0). Due to the periodicity of both the EBG and its eigenvalues, we only need to analyze the bands for the wavevectors in the first Brillouin zone: solutions for wavevectors outside this zone can be related

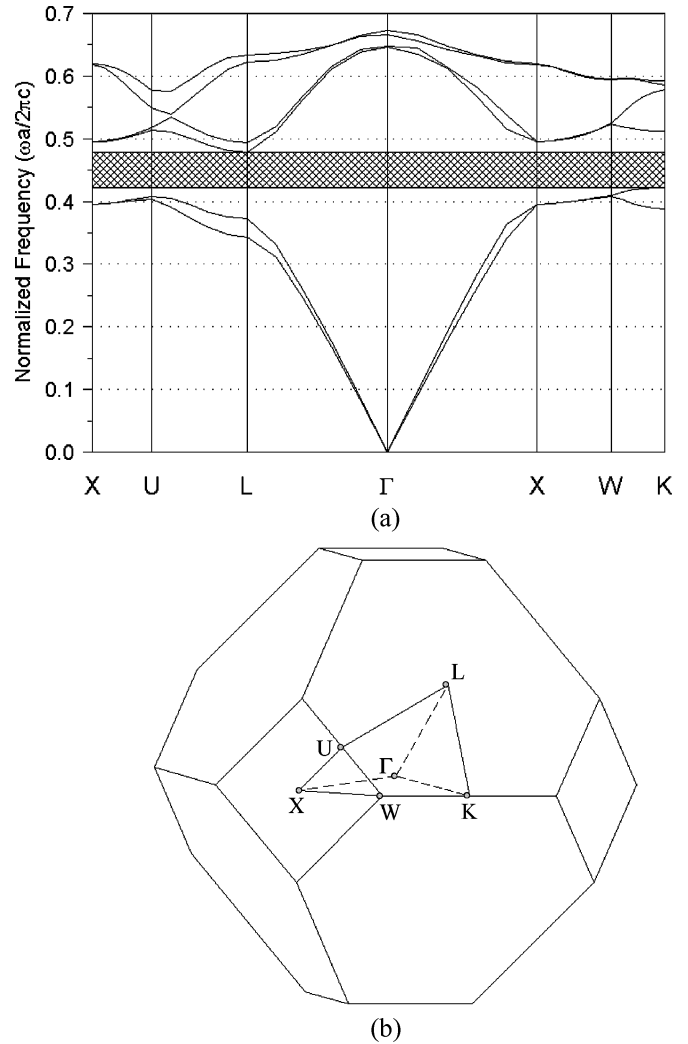


Fig. 2. (a) Band diagram for the woodpile EBG material. The shaded region corresponds to the bandgap of the material, since there are no modes present. (b) Brillouin zone for the fct lattice. The irreducible Brillouin zone is the polyhedron with corners labeled Γ , X, W, K, L, U.

to those within it by integer multiples of the reciprocal lattice vector of the EBG material [1]. There is further redundancy in the first Brillouin zone due to the mirror symmetries of the EBG material, which are removed in the irreducible Brillouin zone. This zone represents the smallest region within the first Brillouin zone where the eigenvalues are unrelated by symmetry.

To confirm the existence of the predicted bandgap in our alumina prototype, we have measured the transmission through it for normal incidence. The experimental setup used in the measurement is shown in Fig. 3. Two microwave horn antennas are placed on either side of the EBG material and the transmission measured from 10 GHz to 15 GHz using a vector network analyzer. The total length of the alumina lattice was 152 mm or 13.6 lattice constants. Measured results presented in Fig. 4 confirm the existence of an EBG from 11.5 to 13.6 GHz. Here we have defined the band edges as the frequencies where the transmission crosses -10 dB. These results are in good agreement with theoretical results of 11.5 to 13.45 GHz obtained using the waveguide simulator method in HFSS [32], which is only valid for normal incidence transmission.

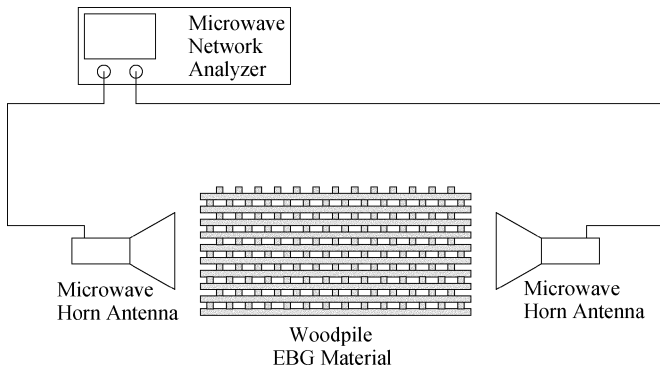


Fig. 3. Experimental setup used to measure normal incidence transmission through the woodpile EBG material.

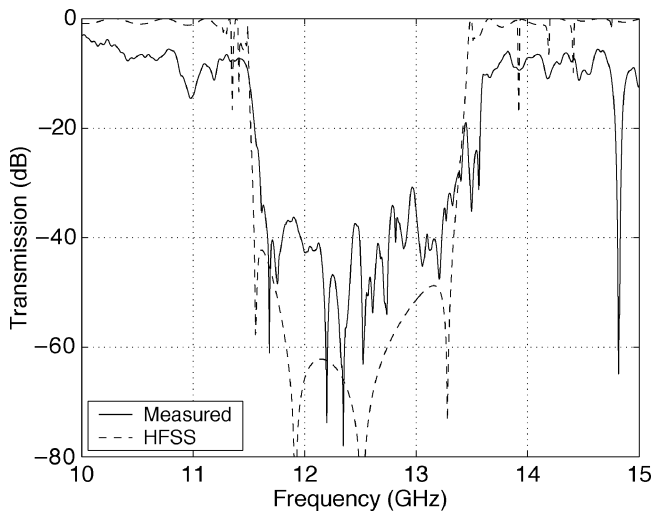


Fig. 4. Measured and computed normal incidence transmission through the woodpile EBG material.

We have also investigated the EBG material's properties as a complex artificial surface, by analyzing a defect resonator that has a resonant frequency within the bandgap. By computing the resonant frequency we can estimate the reflection plane location of the EBG material. The configuration of the defect resonator is shown in Fig. 5(a), and its resonant frequency is obtained by calculating the transmission at normal incidence using HFSS. At the resonant frequency of the defect, the transmission through the structure is 100%, even though the frequency is located in the bandgap. Fig. 5(b) shows the defect resonant frequency as a function of the cavity size, d . Also plotted for reference in this figure is the free-space frequency versus free-space wavelength, which shows when the free-space wavelength is equal to the defect size, d . This occurs at 12.31 GHz, when $d = 24.37$ mm and can be interpreted as the frequency when the EBG material acts as either a perfect magnetic or perfect electric conductor. Examination of the field plots confirms it to be a perfect electric conductor.

For defect sizes less than 24.37 mm, the free-space wavelength is greater than d . This can be interpreted as either a reflection plane that occurs inside the woodpile material, or a reflection coefficient at the air/woodpile interface with a *negative* phase change with respect to a perfect electric conductor. This negative phase change accounts for the additional path length

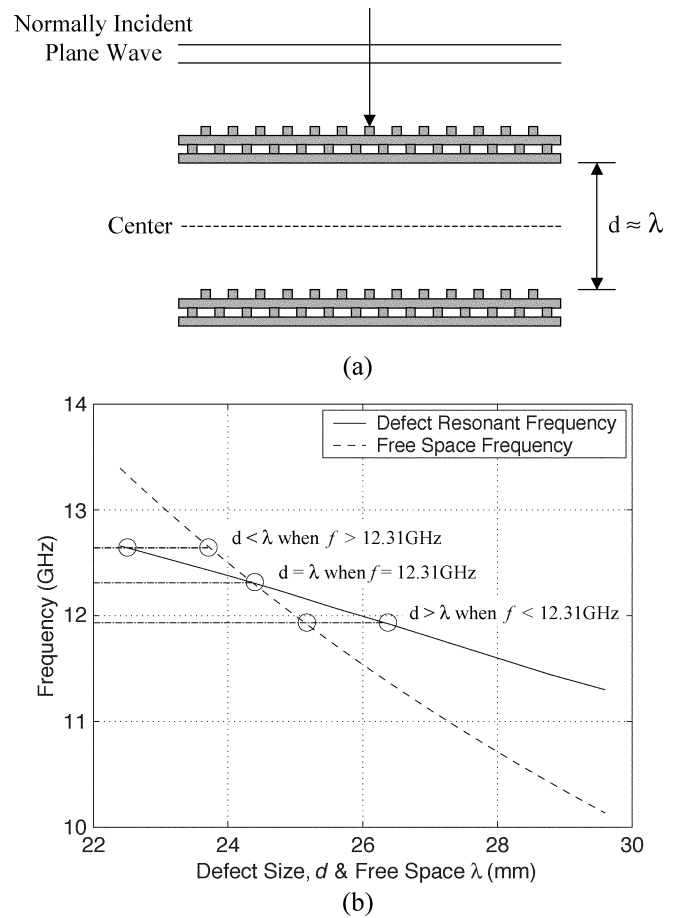


Fig. 5. (a) Configuration of a defect resonator in a woodpile EBG material, showing the defect size, d . (b) Computed resonant frequency for normal incidence transmission through the defect resonator as a function of defect size.

required in the resonator. Conversely, when the defect size is greater than 24.37 mm, the free-space wavelength is less than d and it appears that the reflection plane is located outside the EBG material, or the reflection coefficient at the air/woodpile interface gives a *positive* phase change with respect to a perfect electric conductor. Fig. 5(b) is also used to obtain a good approximation of the operating frequency for the resonator antennas that are discussed in Section III.

III. WOODPILE EBG RESONATOR ANTENNAS

Having confirmed the complete EBG of the woodpile material and examined its properties as a complex artificial surface in Section II, we now turn our attention to two resonator antennas that exploit these material characteristics to create thin high-gain low-loss antennas. Referring to Fig. 5(a), we can create an antenna by placing a metallic ground plane at the center plane of the device. Only half of the entire structure is then required, and the peak radiation will occur in a direction normal to the EBG material and away from the ground plane. For normally incident waves there is 100% transmission from the resonator to free space, whereas obliquely incident waves undergo angle-dependent attenuation. The nature of this coupling to free space creates a highly directional radiation pattern. The operating frequency of the antenna will be determined by the separation between the EBG material and the ground plane, and is close to a

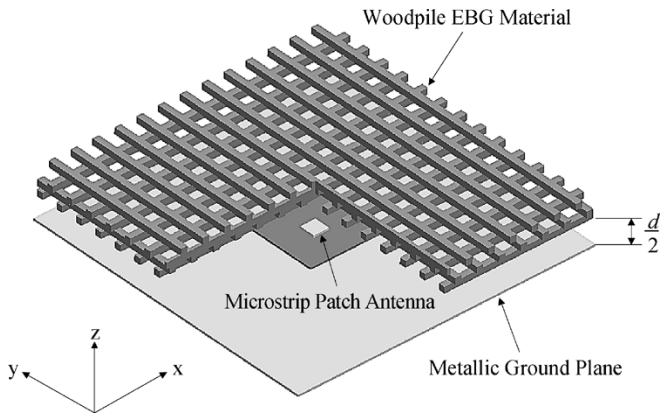


Fig. 6. Cutaway drawing of the woodpile EBG resonator antenna with microstrip patch antenna feed.

half wavelength. The separation for a given operating frequency within the bandgap may be determined from Fig. 5. Since the reflection plane location within the EBG material is frequency dependent, the separation is either slightly smaller or slightly larger than a half wavelength. To couple energy into the resonator formed by the ground plane and EBG material, we have studied two different types of feed antenna: a microstrip patch, and a double slot.

A. Microstrip Patch Antenna Feed

The configuration of the EBG resonator antenna with a microstrip patch feed is shown in Fig. 6. In this figure, one-quarter of the EBG material has been removed to reveal the details of the structure more clearly. The patch antenna is fed from below by a coaxial probe, and mounted on an aluminum ground plane that has an area of $300 \text{ mm} \times 300 \text{ mm}$. The dimensions of the patch are $7.6 \text{ mm} \times 7.6 \text{ mm}$, and it is printed on a 0.787 mm thick Rogers RT/Duroid 5880 substrate. The feed point, where the probe is attached to the patch, is located at the centre of the outside edge of the patch. With the EBG material in place, variation of the feed location does not improve the match of the antenna, as normally is the case for unloaded patch antennas.

Located 11.7 mm above the ground plane is a single cell woodpile EBG material that was analyzed in Section II. As previously mentioned, the cross section of the alumina rods is $3.2 \text{ mm} \times 3.2 \text{ mm}$, and their length is 152 mm . From Fig. 5(b), a half-wavelength separation of 11.7 mm with the metallic image plane corresponds to a full wavelength defect resonant frequency of 12.485 GHz . This is quite close to the measured operating frequency of 12.47 GHz ; the difference may be attributed to the loading effect of the patch antenna.

We have analyzed the resonator antenna using in-house FDTD codes that implement Berenger's perfectly matched layer absorbing boundary conditions [33]. The simulation used a discretization value of 0.4 mm in all three dimensions, which corresponds to 60 cells per wavelength at the operating frequency of the antenna. A comparison of the measured and computed reflection coefficient for the EBG resonator antenna is given in Fig. 7. The wide low-reflection bandwidth shown is most likely due to a traveling wave effect created by the EBG material and ground plane. Although the impedance bandwidth is wide, the practical operating frequency range for

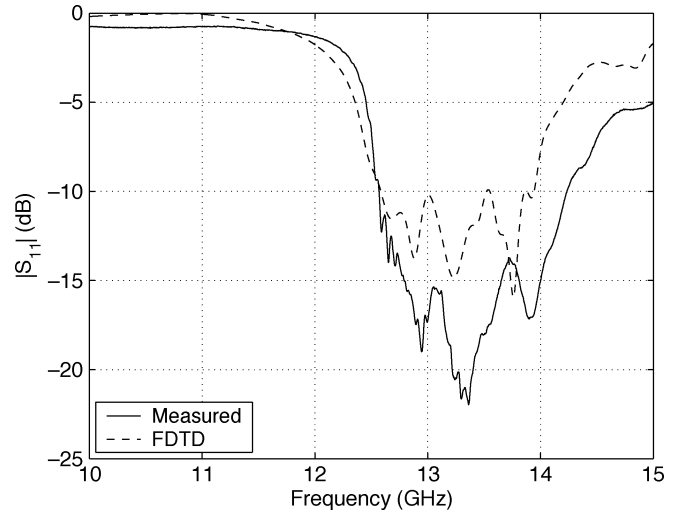


Fig. 7. Measured versus computed reflection coefficient for the woodpile EBG resonator antenna with microstrip patch antenna feed.

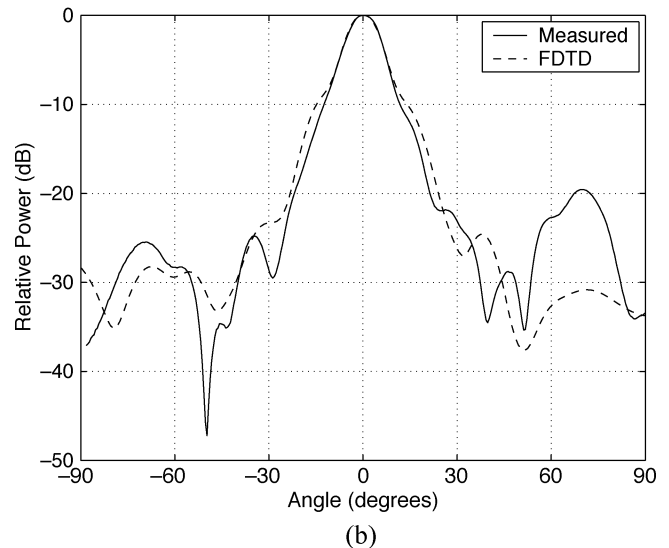
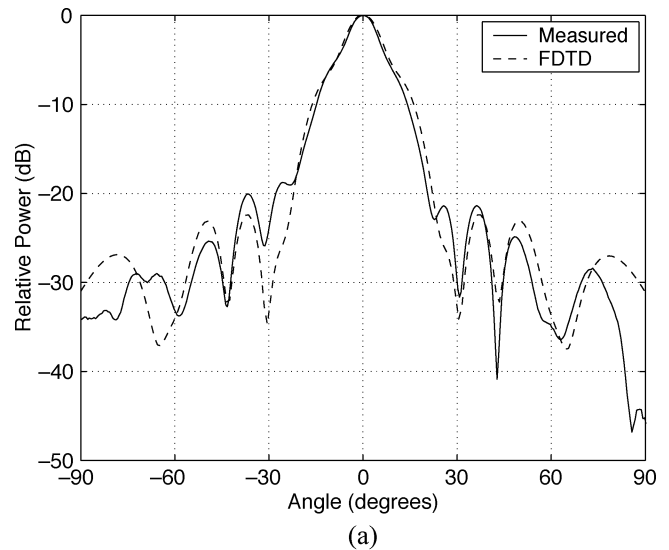


Fig. 8. Measured and computed (a) H-plane and (b) E-plane radiation patterns at 12.47 GHz for the woodpile EBG resonator antenna fed by a microstrip patch.

high directivity is in fact extremely narrow with a value of approximately 1%. Above the operating frequency of 12.47 GHz

TABLE I
MEASURED AND COMPUTED HPBW AND GAIN FOR THE EBG RESONATOR ANTENNA WITH MICROSTRIP PATCH FEED

Frequency (GHz)	E-plane HPBW		H-plane HPBW		Gain (dBi)	
	Measured	Computed	Measured	Computed	Measured	Computed
12.47	11.7°	12.0°	11.0°	12.4°	18.9±1	19.8

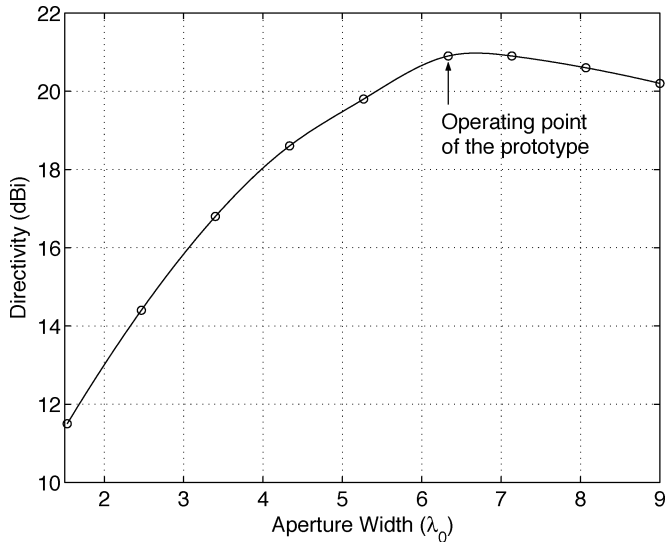


Fig. 9. Computed directivity versus aperture width in wavelengths for the EBG resonator antenna with microstrip patch feed.

the directivity falls in response to dramatic radiation pattern changes with frequency.

Radiation characteristics for the antenna were measured in the 12 m indoor anechoic chamber at CSIRO. Fig. 8 shows the measured versus computed E- and H-plane radiation patterns. There is good agreement between the two patterns, particularly in the depth and location of the sidelobes in the H-plane. In both principal planes, the boresight cross-polarization level is lower than -32 dB. The measured and computed HPBW's for the two principal planes as well as the gain of the antenna are listed in Table I. The directivity of the antenna has been computed from the measured co- and cross-polarized radiation patterns by numerical integration giving 21.7 dB at 12.47 GHz. From the scattering coefficient $|S_{11}|$ of -5.75 dB at 12.47 GHz, the antenna mismatch efficiency is -1.34 dB. The conduction/dielectric efficiency (or ohmic loss) is estimated from the directivity, measured gain and mismatch efficiency to be -1.46 dB or 71%. This is lower than the FDTD computed value of 92%, which neglects the connector and the ground plane losses.

The woodpile resonator antenna has the useful property that changing the area of the aperture modifies its directivity. We have investigated this characteristic numerically using the FDTD method. For the configuration of Fig. 6, we modified the width of the woodpile material and ground plane equally in the x and y directions. The results of this analysis are plotted in Fig. 9. This shows that the directivity varies in a linear manner with aperture width from $1.5\lambda_0$ to $6.5\lambda_0$. Above $6.5\lambda_0$ the directivity begins to reduce slightly, and converges to a value just below the maximum. For the smaller aperture size the level of the sidelobes increase, staying below -10 dB for aperture widths greater than $2.5\lambda_0$.

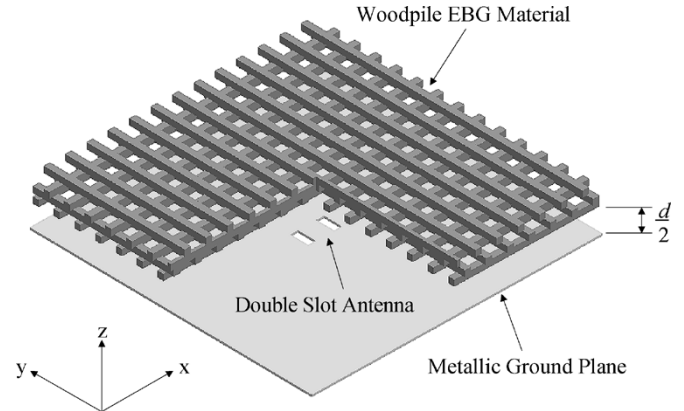


Fig. 10. Cutaway drawing of the woodpile EBG resonator antenna with double slot antenna feed. The slots are fed by a rectangular waveguide at the back of the ground plane.

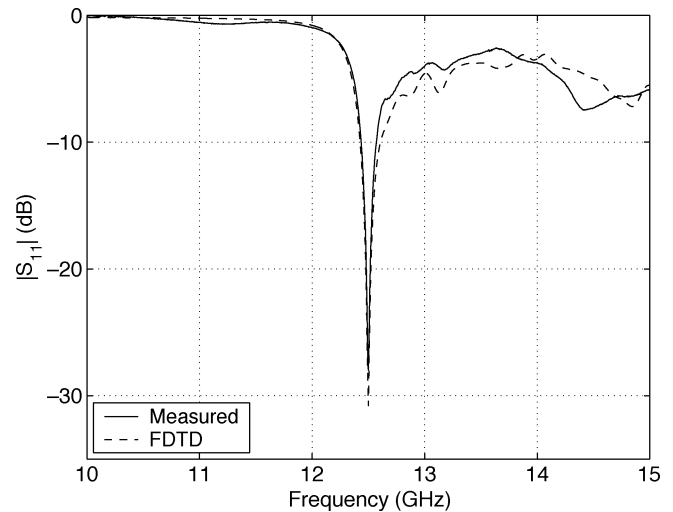


Fig. 11. Measured versus computed reflection coefficient for the woodpile EBG resonator antenna with double slot antenna feed.

B. Double Slot Antenna Feed

The second feed type that has been examined is the double slot antenna; a drawing showing the configuration of the EBG resonator antenna with this type of feed element is shown in Fig. 10. Two rectangular slots have been cut into an aluminum ground plane that is 1 mm thick, with an area of $300 \text{ mm} \times 300 \text{ mm}$. The slots are fed from below the ground plane by a waveguide with a square cross-section that is $19.2 \text{ mm} \times 19.2 \text{ mm}$, which is connected to a waveguide-to-coaxial transition. The dimensions of the slots are $4 \text{ mm} \times 9.6 \text{ mm}$, and the center axis of each slot are separated by 13.6 mm. In this configuration, the woodpile EBG material is placed 11.6 mm above the ground plane to give an operating frequency of 12.5 GHz. From Fig. 5(b) the estimated operating frequency of the antenna is 12.52 GHz. A comparison of the measured reflection coefficient

TABLE II
MEASURED AND COMPUTED HPBW AND GAIN FOR THE EBG RESONATOR ANTENNA WITH DOUBLE SLOT FEED

Frequency (GHz)	E-plane HPBW		H-plane HPBW		Gain (dBi)	
	Measured	Computed	Measured	Computed	Measured	Computed
12.565	13.2°	12.2°	13.3°	13.2°	19.8±1	21.8

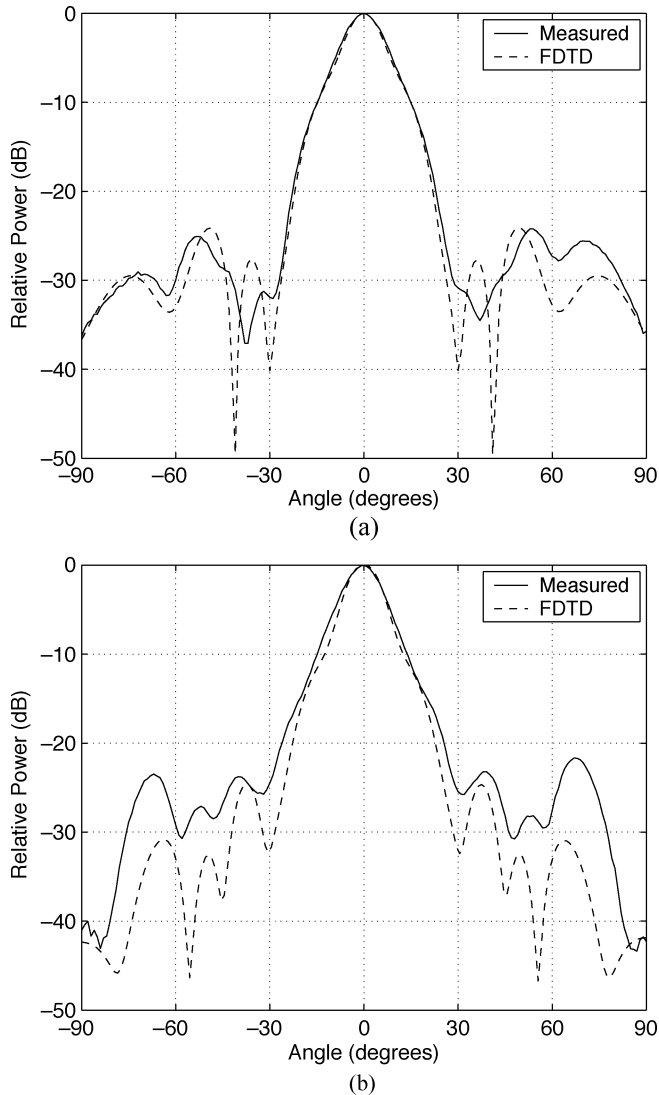


Fig. 12. Measured and computed (a) H-plane and (b) E-plane radiation patterns at 12.565 GHz for the woodpile EBG resonator antenna fed by a double slot.

versus FDTD computed results is presented in Fig. 11. This shows a much clearer, high Q resonance than the microstrip feed and is well matched at the operating frequency. The measured impedance bandwidth extends from 12.435 to 12.565 GHz. This is in good agreement with the FDTD computed bandwidth of 12.426 to 12.607 GHz.

The radiation patterns for this antenna were measured at 12.565 GHz, which is the frequency where the peak gain occurred. The measured E- and H-plane radiation patterns are plotted in Fig. 12 along with the FDTD computed values. The patterns show the directive nature of the antenna, and its low sidelobes. There is a slight discrepancy in the computed sidelobe levels for angles greater than $\pm 60^\circ$. This is most likely

due to diffraction effects from the edges of the ground plane that were not included in the FDTD model. This effect is worse for the E-plane pattern than for the H-plane pattern. Table II lists the measured and computed gain and HPBW's for the two principal planes of the antenna. The measured efficiency of the antenna at 12.565 GHz is 87%, while the FDTD computed value is 93%.

IV. CONCLUSION

A new resonator antenna has been developed from a woodpile EBG material and a metallic ground plane. The antenna has the advantages of high-gain, high efficiency, low sidelobes and a low height. This device exploits the bandgap of the EBG material to create highly directional radiation by virtue of the resonator's angle-dependent transmission properties. Use of the ground plane reduces the overall height of the structure by more than 70% compared to other reported woodpile resonator antennas, leading to a significant decrease in its volume and weight. We demonstrated that the directivity of the antenna can be easily modified, over a given range, by changing the area of the woodpile aperture, and that there is an upper limit on its value. A band diagram was used to confirm the woodpile EBG material's complete bandgap, and its properties as a complex surface were investigated.

Two different methods for feeding the resonator antenna were examined; the microstrip patch element had the advantage of simplicity and compactness while the double slot feed gave the best overall performance. In particular, the reflection coefficient for the double slot is lower at the design frequency, which corresponds to a sharp resonance, and the radiation patterns are similar in the two principal planes. The main disadvantages of the microstrip feed are the poor reflection coefficient at the operating frequency of the antenna and lower measured efficiency due to the additional losses of the probe and microstrip patch. For the double slot feed the main disadvantage is the additional complexity resulting from the waveguide used to deliver energy to the slots. The measured gain, radiation patterns, reflection coefficient and efficiency were predicted reasonably accurately for both feed configurations using the FDTD method. Future work will concentrate on combining the advantages of both the patch and double slot through the use of stripline slot feeds.

ACKNOWLEDGMENT

The authors thank Mr. K. Smart of the CSIRO ICT Centre for assisting with the measurements and the Australian Centre for Advanced Computing and Communications (AC3) for providing access to the supercomputing facilities.

REFERENCES

- [1] J. D. Joannopoulos, R. D. Meade, and J. N. Winn, *Photonic Crystals: Molding the Flow of Light*. Princeton, NJ: Princeton Univ. Press, 1995.

- [2] P. de Maagt, R. Gonzalo, Y. C. Vardaxoglou, and J. M. Baracco, "Electromagnetic bandgap antennas and components for microwave and (sub)millimeter wave applications," *IEEE Trans. Antennas Propag.*, vol. 51, no. 10, pp. 2667–2677, Oct. 2003.
- [3] E. R. Brown, C. D. Parker, and E. Yablonovitch, "Radiation properties of a planar antenna on a photonic-crystal substrate," *J. Opt. Soc. Amer. B.*, vol. 10, pp. 404–407, Feb. 1993.
- [4] S. D. Cheng, R. Biswas, E. Ozbay, S. McCalmont, G. Tuttle, and K. M. Ho, "Optimized dipole antennas on photonic band-gap crystals," *Appl. Phys. Lett.*, vol. 67, no. 23, pp. 3399–3401, Dec. 1995.
- [5] M. M. Sigalas, R. Biswas, Q. Li, D. Crouch, W. Leung, R. Jacobs-Woodbury, B. Lough, S. Nielsen, S. McCalmont, G. Tuttle, and K. M. Ho, "Dipole antennas on photonic band-gap crystals—experiment and simulation," *Microwave Opt. Technol. Lett.*, vol. 15, no. 3, pp. 153–158, Jun. 1997.
- [6] D. Sievenpiper, L. Zhang, R. F. J. Broas, N. G. Alexopoulos, and E. Yablonovitch, "High-impedance electromagnetic surfaces with a forbidden frequency band," *IEEE Trans. Microw. Theory Tech.*, vol. 47, no. 11, pp. 2059–2074, Nov. 1999.
- [7] R. Gonzalo, I. Eterra, C. M. Mann, and P. de Maagt, "Radiation properties of terahertz dipole antenna mounted on photonic crystal," *Electron. Lett.*, vol. 37, no. 10, pp. 613–614, May 2001.
- [8] F. Yang and Y. Rahmat-Samii, "Reflection phase characterizations of the EBG ground plane for low profile wire antenna applications," *IEEE Trans. Antennas Propag.*, vol. 51, no. 10, pp. 2691–2703, Oct. 2003.
- [9] W. Y. Leung, R. Biswas, S. D. Cheng, M. M. Sigalas, J. S. McCalmont, G. Tuttle, and K. M. Ho, "Slot antennas on photonic band gap crystals," *IEEE Trans. Antennas Propag.*, vol. 45, no. 8, pp. 1569–1570, Aug. 1997.
- [10] R. Coccioli, F. R. Yang, K. P. Ma, and T. Itoh, "Aperture-coupled patch antenna on UC-PBG substrate," *IEEE Trans. Microw. Theory Tech.*, vol. 47, no. 11, pp. 2123–2130, Nov. 1999.
- [11] R. Gonzalo, P. de Maagt, and M. Sorrolla, "Enhanced patch-antenna performance by suppressing surface waves using photonic-bandgap substrates," *IEEE Trans. Microw. Theory Tech.*, vol. 47, no. 11, pp. 2131–2138, Nov. 1999.
- [12] J. S. Colburn and Y. Rahmat-Samii, "Patch antennas on externally perforated high dielectric constant substrates," *IEEE Trans. Antennas Propag.*, vol. 47, no. 12, pp. 1785–1794, Dec. 1999.
- [13] F. Yang and Y. Rahmat-Samii, "Microstrip antennas integrated with electromagnetic band-gap (EBG) structures: a low mutual coupling design for array applications," *IEEE Trans. Antennas Propag.*, vol. 51, no. 10, pp. 2936–2946, Oct. 2003.
- [14] T. H. Liu, W. X. Zhang, M. Zhang, and K. F. Tsang, "Low profile spiral antenna with PBG substrate," *Electron. Lett.*, vol. 36, no. 9, pp. 779–780, Apr. 2000.
- [15] F. Yang and Y. Rahmat-Samii, "A low-profile circularly polarized curl antenna over an electromagnetic bandgap (EBG) surface," *Microwave Opt. Technol. Lett.*, vol. 31, no. 4, pp. 264–267, Nov. 2001.
- [16] M. P. Kesler, J. G. Maloney, and B. L. Shirley, "Antenna design with the use of photonic band-gap materials as all-dielectric planar reflectors," *Microwave Opt. Technol. Lett.*, vol. 11, no. 4, pp. 169–174, Mar. 1996.
- [17] G. S. Smith, M. P. Kesler, and J. G. Maloney, "Dipole antennas used with all-dielectric, woodpile photonic band-gap reflectors: gain, field patterns, and input impedance," *Microwave Opt. Technol. Lett.*, vol. 21, no. 3, pp. 191–196, May 1999.
- [18] M. Thèvenot, A. Reineix, and B. Jecko, "A dielectric photonic parabolic reflector," *Microwave Opt. Technol. Lett.*, vol. 21, no. 6, pp. 411–414, Jun. 1999.
- [19] D. F. Sievenpiper, J. H. Schaffner, H. J. Song, R. Y. Loo, and G. Tangonan, "Two-dimensional beam steering using an electrically tunable impedance surface," *IEEE Trans. Antennas Propag.*, vol. 51, no. 10, pp. 2713–2722, Oct. 2003.
- [20] H. Y. Yang and N. G. Alexopoulos, "Gain enhancement methods for printed circuit antennas through multiple superstrates," *IEEE Trans. Antennas Propag.*, vol. 35, no. 7, pp. 860–863, Jul. 1987.
- [21] C. Serier, C. Cheype, R. Chantalat, M. Thèvenot, T. Monédière, A. Reineix, and B. Jecko, "1-D photonic bandgap resonator," *Microwave Opt. Technol. Lett.*, vol. 29, no. 5, pp. 312–315, Jun. 2001.
- [22] M. Thèvenot, M. S. Denis, A. Reineix, and B. Jecko, "Design of a new photonic cover to increase antenna directivity," *Microwave Opt. Technol. Lett.*, vol. 22, no. 2, pp. 136–139, Jul. 1999.
- [23] C. Cheype, C. Serier, M. Thèvenot, T. Monédière, A. Reineix, and B. Jecko, "An electromagnetic bandgap resonator antenna," *IEEE Trans. Antennas Propag.*, vol. 50, no. 9, pp. 1285–1290, Sep. 2002.
- [24] R. Biswas, E. Ozbay, B. Temelkuran, M. Bayindir, M. M. Sigalas, and K.-M. Ho, "Exceptionally directional sources with photonic-bandgap crystals," *J. Opt. Soc. Amer. B.*, vol. 18, no. 11, pp. 1684–1689, Nov. 2001.
- [25] A. R. Weily, K. P. Esselle, B. C. Sanders, and T. S. Bird, "Antennas based on 2-D and 3-D electromagnetic bandgap materials," in *IEEE AP-S Int. Symp. Dig.*, 2003, pp. 847–850.
- [26] S. Enoch, B. Gralak, and G. Tayeb, "Enhanced emission with angular confinement from photonic crystals," *Appl. Phys. Lett.*, vol. 81, no. 9, pp. 1588–1590, Aug. 2002.
- [27] I. Bulu, H. Caglayan, and E. Ozbay, "Highly directive radiation from sources embedded inside photonic crystals," *Appl. Phys. Lett.*, vol. 83, no. 16, pp. 3263–3265, Oct. 2003.
- [28] S. Enoch, G. Tayeb, P. Sabouroux, N. Guérin, and P. Vincent, "A metamaterial for directive emission," *Phys. Rev. Lett.*, vol. 89, no. 21, p. 213 902, Nov. 2002.
- [29] A. R. Weily, K. P. Esselle, and B. C. Sanders, "Photonic crystal horn and array antennas," *Phys. Rev. E*, vol. 68, no. 1, p. 16 609, Jul. 2003.
- [30] K. M. Ho, C. T. Chan, C. M. Soukoulis, R. Biswas, and M. M. Sigalas, "Photonic band gaps in three dimensions: new layer-by-layer periodic structures," *Solid State Commun.*, vol. 89, pp. 413–416, 1994.
- [31] RSOFTEC Design Group Inc., BandSOLVE 1.0 User Manual, Ossining, NY, 2002.
- [32] Ansoft Corporation, High Frequency Structure Simulator 8.5 User Manual, Pittsburgh, PA, 2001.
- [33] A. Taflov and S. C. Hagness, *Computational Electrodynamics: The Finite-Difference Time-Domain Method*, 2nd ed. Boston, MA: Artech House, 2000.



Andrew R. Weily (S'96–M'01) received the B.E. degree in electrical engineering from the University of New South Wales, Sydney, Australia, in 1995, and the Ph.D. degree in electrical engineering from the University of Technology of Sydney (UTS), Sydney, Australia, in 2001.

From 2000 to 2001, he was a Research Assistant at UTS, working on medical applications of microwave antennas. He is currently an Australian Research Council (ARC) Postdoctoral Research Fellow with the Department of Electronics, Macquarie University, Sydney, New South Wales, Australia. His research interests are in the areas of photonic crystal antennas and waveguide components, dielectric resonator filters, and numerical methods in electromagnetics.



Levente Horvath received the B.Sc. (Hons.) and the Ph.D. degrees in physics from Macquarie University, Sydney, New South Wales, Australia, in 1996 and 2002, respectively.

From 2003 to 2004, he was a Research Associate at Macquarie University working on microwave antennas and waveguides in photonic crystals. He is currently a Research Fellow at the University of Auckland, Auckland, New Zealand. His research interests include quantum optics, cavity QED, photonic crystal antennas, and computational methods for many body problems and entangled systems.



Karu P. Esselle (M'92–SM'96) received the B.Sc. degree (First Class Honors) in electronic and telecommunication engineering, from the University of Moratuwa, Sri Lanka, in 1983, and the M.A.Sc. and Ph.D. degrees in electrical engineering from the University of Ottawa, Canada, in 1987 and 1990, respectively.

From 1984 to 1985, he was an Assistant Lecturer at the University of Moratuwa. He was a Research Assistant at the University of Ottawa, Canada, from 1987 to 1990, and a Canadian Government Laboratory Visiting Postdoctoral Fellow from 1990 to 1992. In 1992, he joined Macquarie University, Sydney, Australia, where he is currently an Associate Professor in electronics. He was a Visiting Professor at the University of Victoria, Canada, in 1996/97 and a Visiting Scientist in the Division of Telecommunications and Industrial Physics, CSIRO, New South Wales, Australia, in 2002. He is currently the Director of Postgraduate Research in the Division of Information and Communication Sciences and the Director of the Centre for Electromagnetic and Antenna Engineering (CELANE) at Macquarie University, Sydney, Australia. Since 2002, he was involved with research grants and contracts worth over two million dollars. At present, he is leading the establishment of a national antenna testing facility funded by the Australian Research Council, Macquarie University, and six other collaborating institutions. His industry experience includes full-time employment as a Faculty Hire Design Expert by the Hewlett Packard Laboratory, Palo Alto, CA, and several consultancies for local and international companies including Cisco Systems and Locata Corporation. He serves as a Research Grant Assessor to several organizations including the Australian Research Council, Netherlands Organization for Scientific Research, and Hong-Kong University Grants Commission. He is a regular referee for nearly all international journals in his area. He has coauthored over 100 papers, including four invited book chapters. His current research interests include multiband antennas for wireless local area networks, photonic crystals and PBG/EBG structures, microwave antennas based on electromagnetic bandgap, smart antenna systems, theoretical methods in electromagnetics, metamaterials and applications, antennas for radio astronomy, broad-band antennas, dielectric-resonator and hybrid antennas, and enhanced FDTD methods for thin metal films, strips, and printed circuits. He collaborates with prestigious research groups in the world. His research has been sponsored by many organizations that include the Australian Research Council, the Department of Industry, Science and Tourism, Australian Telecommunications and Electronics Research Board, Macquarie University and industry.

Dr. Esselle was awarded a Canadian Commonwealth Scholarship from 1985 to 1990 and an International Scientific Radio Union (URSI) Young Scientist Award in 1990. He was an organizer and the Publicity Chair of the 2000 Asia-Pacific Microwave Conference. He has also served on Technical Program Committees or International Committees for many conferences including IEEE AP-S Int. Symp., EUROEM, APMC, PIERS, AMEREM, Netherlands Organization for Scientific Research, IASTED, ARP, and DSPCS, and organized special sessions on PBG/EBG Structures in IEEE AP-S and PIERS. From 1999 to 2002, he was Chair of the IEEE New South Wales MTT/AP Joint Chapter of which he is currently Secretary and Treasurer, Chair of the Educational Activities Committee of the IEEE NSW Section, and a Member of the IEEE NSW Executive Committee.



Barry C. Sanders received the B.Sc. (Hons.) degree in physics from the University of Calgary, Calgary, ON, Canada, in 1984, and the Diploma in mathematical physics and the Ph.D. degree in physics from Imperial College, University of London, London, U.K., in 1986 and 1987, respectively.

Currently, he is the iCORE Professor of quantum information science at the University of Calgary, Alberta, ON, Canada, the Director of Calgary's Institute for Quantum Information Science, as well as an Adjunct Professor of quantum information science at Macquarie University, Sydney, New South Wales, Australia. His research interests are in quantum information science and quantum optics, including the radiative properties of photonic crystals in both the optical and microwave domains.

Dr. Sanders is a Fellow of the Institute of Physics (U.K.), a Fellow of the Optical Society of America, a Fellow of the Australian Institute of Physics, an Associate of the Canadian Institute for Advanced Research, and Past-President of the Australian Optical Society.



Trevor S. Bird (S'71–M'76–SM'85–F'97) received the B.App.Sc., M.App.Sc., and Ph.D. degrees from the University of Melbourne, Melbourne Australia, in 1971, 1973, and 1977, respectively.

From 1976 to 1978, he was a Postdoctoral Research Fellow at Queen Mary College, University of London, London, U.K., followed by five years as a Lecturer in the Department of Electrical Engineering, James Cook University, North Queensland, Australia. During 1982 and 1983, he was a Consultant at Plessey Radar, U.K., and in December

1983 he joined CSIRO, Sydney, Australia. He has held several positions with CSIRO and is currently Chief Research Scientist and Research Leader of the Electromagnetics and Antennas Group, CSIRO ICT Centre. He is also an Adjunct Professor at Macquarie University, Sydney, Australia. He has published widely in the area of antennas, waveguides, electromagnetics, and satellite communication antennas, and holds eight patents.

Dr. Bird is a Fellow of the Australian Academy of Technological and Engineering Sciences, the Institution of Electrical Engineers (IEE), London, U.K., and Engineers Australia. In 1988, 1992, 1995, and 1996 he received the John Madsen Medal of the Institution of Engineers, Australia, for the best paper published annually in the *Journal of Electrical and Electronic Engineering*, Australia, and in 2001 he was co-recipient of the H.A. Wheeler Applications Prize Paper Award of the IEEE Antennas and Propagation Society. He was awarded a CSIRO Medal in 1990 for the development of an Optus-B satellite spot beam antenna and again in 1998 for the multibeam antenna feed system for the Parkes radio telescope. He received an IEEE Third Millennium Medal in 2000 for Outstanding Contributions to the IEEE New South Wales Section. Engineering projects that he played a major role in were given awards by the Society of Satellite Professionals International (New York) in 2004, The Institution of Engineers, Australia, in 2001, and the Communications Research Laboratory, Japan, in 2000. In 2003, he was awarded a Centenary Medal for service to Australian society in telecommunications and also named Professional Engineer of the Year by the Sydney Division of The Institution of Engineers Australia. In 2004, he was listed in the *Top 100 Australia's Most Influential Engineers* by Engineers Australia. He was a Distinguished Lecturer for the IEEE Antennas and Propagation Society from 1997 to 1999, Chair of the New South Wales joint AP/MTT Chapter from 1995 to 1998, and again in 2003, Chairman of the 2000 Asia Pacific Microwave Conference, Vice-chair and Chair of the New South Wales Section in 1999 to 2000 and 2001 to 2002, respectively, and Associate Editor of the IEEE TRANSACTIONS ON ANTENNAS AND PROPAGATION from 2001 to 2004. He is currently Editor-in-Chief of the IEEE TRANSACTIONS ON ANTENNAS AND PROPAGATION, and a Member of Adcom of the Antennas and Propagation Society.